TABLE 2
Genes Changed of Their Expression in At Least Four Chemical-Administered Rats

Gene name			
Up regulation	Genbank ID	Common name	Pass chemicals
Heme oxygenase	NM_012580	Hmox1	5
Diaphorase (NADH/NADPH)	J02679	Dia4	5
T-cell death associated gene	NM_017180	Tdag	5
P-glycoprotein/multidrug resistance 1	AF257746	Pgy1	5
Janus kinase 2 (a protein tyrosine kinase)	U13396	Jak2	4
Gro	NM_030845	Gro1	4
Heat shock cognate protein 70	NM_024351	Hsc70	4
RNA polymerase I (127 kDa subunit)	NM_031773	Rpo1-2	4
Small inducible gene JE	Scya2	Scya2	4
Thioredoxin reductase 1	NM_031614	Txnrd1	4
Heat shock protein 70-1	Z75029	Hspa1a	4
Lysozyme	NM_012771	Lyz	4
mRNA for alpha-2u globulin-related protein	X13295	Lcn2	4
Aldose-reductase-like protein MVDP/AKR1-B7 mRNA, complete cds	AF182168	Rn.32702	4
Interferon inducible protein 10 (IP-10) mRNA, complete cds	U22520	Rn.10584	4
VESP11 mRNA for vascular endothelial cell specific protein 11, complete cds	AB027561	Rn.65187	4
Aldolase A, fructose-bisphosphate	NM_012495	Aldoa	4
Caspase 3, apoptosis related cysteine protease (ICE-like cysteine protease)	U49930	Casp3	4
Potassium channel, subfamily K, member 3	U02316	Kcnk3	4
Cyclin G1	X70871	Ccng1	4
DNA-damage-inducible transcript 1	NM_024127	Gadd45a	4
Glutathione synthetase gene	L38615	Gss	4
3-hydroxy-3-methylglutaryl-Coenzyme A reductase	X55286	Hmgcr	4
Activating transcription factor 3	NM_012912	Atf3	4
Cathepsin L	Y00697	Ctsl	4
Down regulation			
sulfotransferase family 1A, phenol-preferring, member 2	NM_031732	Sult1a2	5
Rattus norvegicus NADPH oxidase 4 mRNA, complete cds	AY027527	Rn.14744	5
Gastrin	NM_012849	Gas	5
Stearoyl-CoA desaturase-1 (SCD-1)	NM_139192	Scd1	5
Sulfonylurea receptor	NM_013039	Sur	5
Thyroid stimulating hormone receptor	NM_012888	Tshr	5
Thyroid hormone receptor	X12744	Thra	5
Brain digoxin carrier protein mRNA, complete cds	U88036	Rn.5641	5
Neurotrophin 5 (neurotrophin 4/5)	NM_013184	Ntf5	4
Ornithine aminotransferase	NM_022521	Oat	4
Triadin 1	AJ243304	Trdn	4
Neuropeptide Y5 receptor	U66274	Npy5r	4
Transforming growth factor beta stimulated clone 22	NM_013043	Tgfb1i4	4
Retinoblastoma 1 (including osteosarcoma)	L07126	Rb1	4
mRNA for V1a arginine vasopressin receptor	Z11690	Rn.32282	4
Cytochrome P450 2D18 mRNA, complete cds	U48220	Cyp2d18	4
L-3-hydroxyacyl-CoA dehydrogenase precursor (HAD) mRNA, complete cds	AF095449	Rn.17172	4
ATPase inhibitor (rat mitochondrial IF1 protein)	AF368860	Atpi	4
Diazepam binding inhibitor (GABA receptor modulator, acyl-Coenxyme A binding protein)	M20268	Dbi	4
Expressed in non-metastatic cells 3, protein (nucleoside diphosphate kinase)	AY017337	Nme3	4
Insulin-like growth factor-I mRNA, 3′ end	X06108	Rn.6282	4
Estrogen sulfotransferase	NM_012883	Ste	4
Galanin receptor 3	NM_019173	Galr3	4
Pim-1 oncogene	X63675	Pim1	4
Carbonic anhydrase 2	X58294	Ca2	4
CL1BA protein	U72487	CL1BA	4
Epidermal growth factor	U04842	Egf	4

Note. Gene whose expressions were altered more than 2.0-fold at the maximal toxic time by at least four of the five chemicals. APAP: 12 h; BB: 24 h; CT: 6 h; DMN: 48 h; TA: 24 h.

respectively. In both cluster analyses, 6 and 12 h of the CT-administered groups and 24 h of the TA-administered groups were sorted in a similar cluster.

Gene Expression Profiles and Maximal Toxic Time

The peak profiles of 10 up- or down-regulated genes in Table 2 were each overlapped at the maximal toxic times (Fig. 2). The expression profiles in each of the chemical-administered groups showed similar patterns at all the time points investigated in the present study.

To confirm the gene expression profiles of DNA microarray as shown in Figure 2, real-time RT-PCR was performed (Fig. 3). The expression profiles of all five genes were almost the same as those of DNA microarray. The extent of these gene expressions was higher than that of DNA microarray.

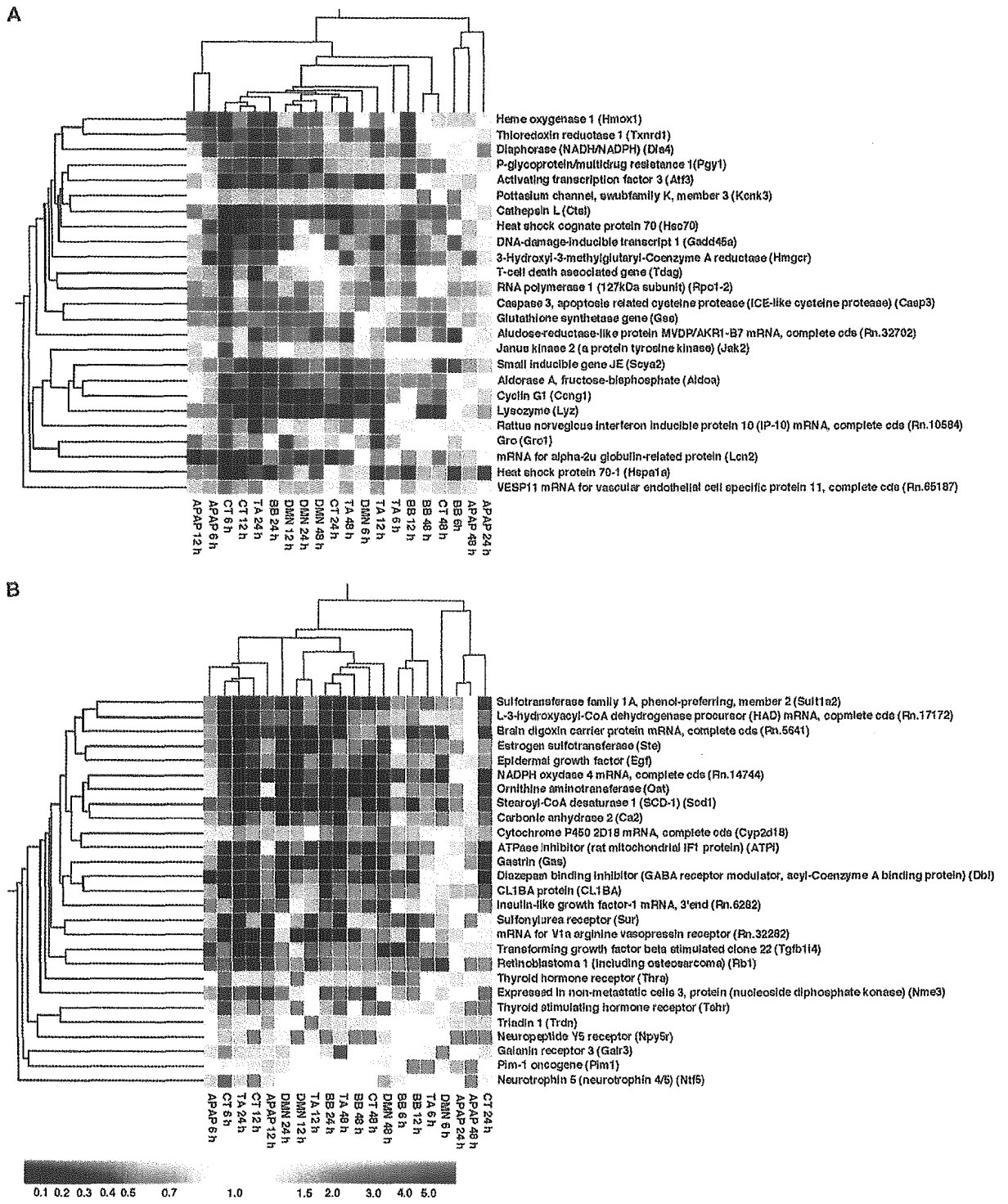

FIG. 1. Two-way hierarchical cluster images of genes whose expressions were altered more than 2-fold at the maximal toxic times by at least four chemicals. The results of hierarchical cluster analyses are shown with a dendrogram for (A) 25 up-regulated genes and (B) 27 down-regulated genes listed in Table 2. Gene expression data are expressed as fold of control values, and the range of change represented by colors at the bottom of the cluster images. The expression pattern of each gene is displayed here as a horizontal strip.

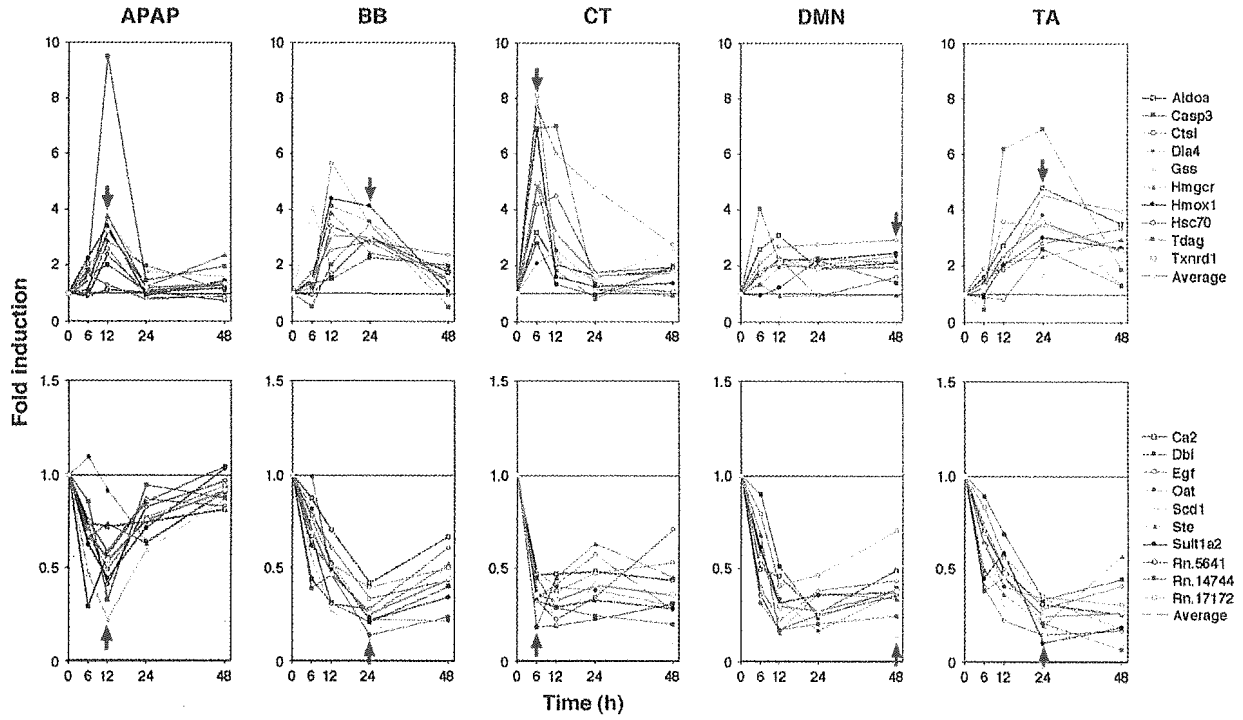

FIG. 2. Time-dependent changes of the expressions of 20 representative genes in Table 2. The peaks of the expression in up- or down-regulated genes were overlapped with the maximal toxic times examined in the present study. Red arrows indicate the maximal toxic time in each chemical-administrated group estimated from the change of biochemical markers. Official gene name is described in Table 2.

QT Clustering for Minimal Correlation

In order to estimate the majority of the gene expression profiles, QT clustering analysis was performed. In this process, we used the GeneSpring QT clustering algorism. The analysis setting for the minimal cluster size was 100 genes, and the minimal correlation coefficient was 0.5 for the Rat Drug Response Chip containing 1,097 genes. Probes with a certain expression level higher than 0.01 in all the administered samples (759 of 1,097 genes) were used. In all groups, the up-regulated and down-regulated types of clusters were identified and expressed as average values (Fig. 4A). In the up-regulated type cluster, the APAP-, BB-, CT-, DMN-, and TA-administered groups contained 109, 105, 143, 139, and 153 genes, respectively (upper part of Fig. 4A). The down-regulated type clusters of the APAP-, BB-, CT, DMN-, and TA-administered groups contained 122, 159, 180, 144, and 163 genes, respectively (lower part of Fig. 4A). As a result, all clusters except those of DMN reflected the maximal toxic time.

In order to confirm the data with the Rat Drug Response Chip, analysis with Agilent Rat cDNA microarray kit G4105A was performed only in the APAP-administered group. QT clustering was also performed, and the analysis setting for the minimal cluster size was 1,000 genes, and the minimal correlation coefficient was 0.68. Probes with a certain expression level higher than 0.01 in all administered samples (14,474 of 14,815 genes) were used. Up-regulated and down-regulated type clusters contained 1,058 and 1,106 genes, respectively, and were expressed as mean values (Fig. 4B). As expected, both clusters of APAP showed almost the same profiles as those of the Rat Drug Response Chip.

Genes Appeared in All Five of the Chemical-Administered Groups

For further analysis, the gene expression profiles identified in the gene clusters of all chemicals in Figure 4A were displayed. Three genes were contained in all the up-regulated type clusters and 17 genes in the down-regulated type clusters of all the chemical-administered groups as shown in Figure 4. The expression profiles of 17 down-regulated genes are shown in Figure 4A. The blue lines indicate the expression profiles of the genes that appeared not only in Figure 2 but also in Figure 4. The expression profiles of the genes that appeared in all chemical groups but only in Figure 4 are indicated by black lines. The three common genes in the up-regulated type cluster were not listed in Figure 2 (data not shown). In the down-regulated type cluster, eight genes of all the regulated groups were also listed in Figure 2. The 3 up-regulated and 17 down-regulated genes were analyzed in the following QT clustering.

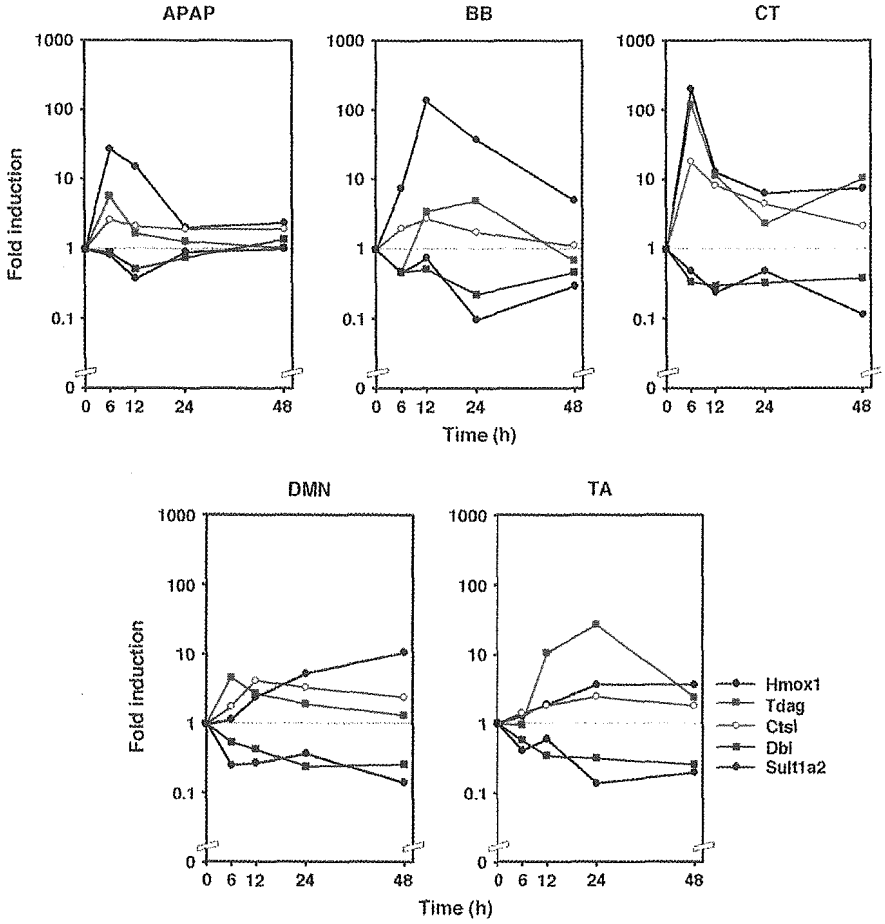

FIG. 3. Real-time RT-PCR analysis of the expression of the representative genes. Total RNA samples from four rats were pooled and used for real-time RT-PCR analysis. This figure contains the representative three up-regulated and two down-regulated genes as shown in Figure 2. Official gene name is described in Table 2.

QT Clustering for the Genes That Appeared in at Least Four of Five Chemical-Administered Groups

For further analysis, the genes that appeared in at least four of the five chemical-administered groups were analyzed. Thirty-seven genes were identified in the up-regulated type cluster and 60 genes in the down-regulated type cluster, as shown in Figure 4. In the up-regulated type cluster, 7 of 37 genes were overlapped with the genes of the up-regulated groups shown in Figure 2. In the down-regulated type cluster, all genes of the down-regulated groups in Figure 2 were overlapped. Further QT clustering was performed using the 37 up-regulated or 60 down-regulated genes identified in Figure 4A. The analysis setting for the minimal cluster size was 10 genes and the minimal correlation coefficient was 0.65. Twenty-two of 37 genes were identified as the up-regulated type cluster, and 44 of 60 genes as the down-regulated type cluster. The profiles of the 22 and 44 identified genes and the average profile are shown in Figures 5B and 5C, respectively. The expression profiles of the genes that also appeared in Figure 2 are indicated by blue lines. The expression profiles of the clustered gene that did not appear in Figure 2 are indicated by black lines. Seven of 10 genes in the up-regulated group in Figure 2 and all 10 genes in the down-regulated group in Figure 2 were overlapped as a result of the clustering (Figs. 5B and 5C). As shown in Figures 5A, 5B, and 5C, the average up-regulated or down-regulated peaks were correlated with the maximal toxic times.

DISCUSSION

Gene expression changes have been used routinely to obtain specific mechanistic information concerning the type of action of a toxicant. Toxicogenomics is an approach that applies microarray technology to toxicological evaluation paradigms.

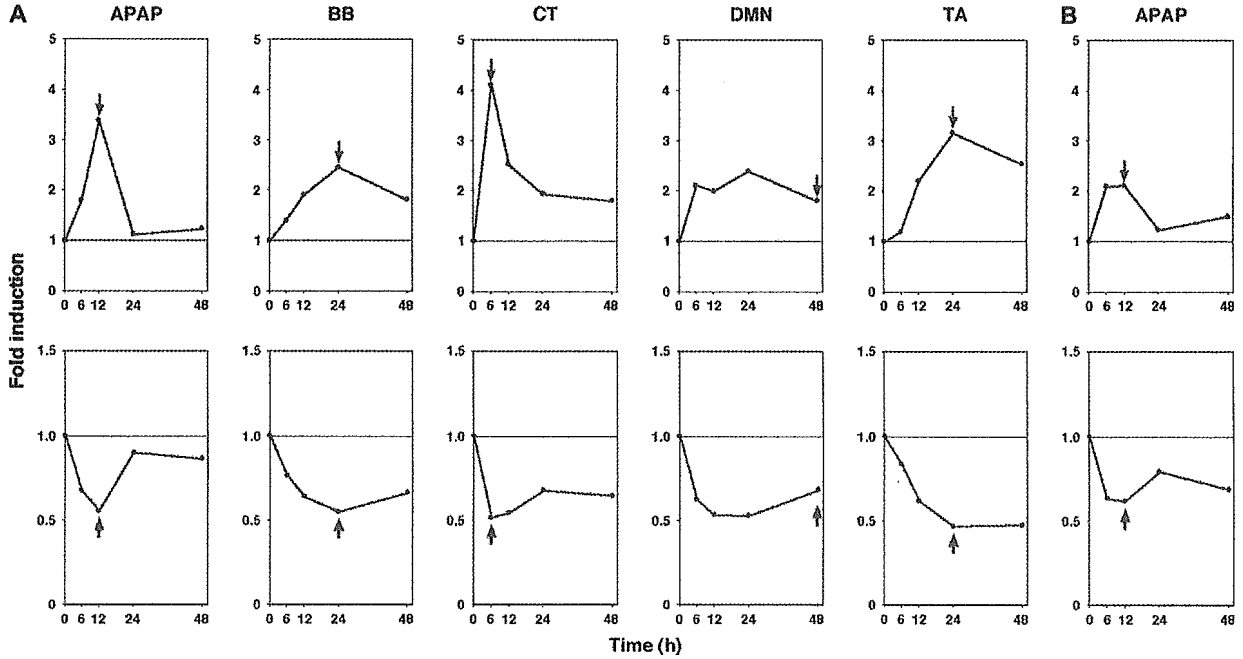

FIG. 4. QT clustering analysis of hepatic gene expression in rats administered the five chemicals. (A) The clustering setting for the correlation coefficient was 0.5 and contained more than 100 genes. The method for QT clustering analysis was described in Materials and Methods. Each figure shows an expression profile using the average of the clustered genes. Arrows indicate the maximal toxic time in each chemical-administered group estimated from the change of biochemical markers. In the upper group, the APAP, BB, CT, DMN, and TA clusters contained 109, 105, 143, 139, and 153 genes, respectively. In the lower group, the APAP, BB, CT, DMN, and TA clusters contained 122, 159, 180, 144, and 163 genes, respectively. (B) QT clustering analysis in APAP-administered rats performed using Agilent Rat cDNA microarray kit G4105A. The clustering setting for the correlation coefficient was 0.68 and contained more than 1,000 genes. The upper cluster contained 1,058 genes, and the lower cluster contained 1,106 genes.

Microarrays are now available that contain huge numbers of genes, even those whose functions are not clear, and the effects of a chemical on the gene expression cannot be assessed with a single microarray experiment.

In this study, we evaluated five typical hepatotoxic chemicals these were thought to cause zone-3 necrosis (Zimmerman, 1999). The dose levels of APAP (Price and Jollow, 1982; Sato and Izumi, 1989), BB (Chakrabarti and Brodeur, 1984), CT (Theocharis *et al.*, 2001), DMN (Asakura *et al.*, 1998), and TA (Wang *et al.*, 2000; Zaragoza *et al.*, 2000) were selected based on their association with detectable hepatotoxicity as previously reported. These data confirmed that the hepatotoxicity models of all the chemical-administered groups were successfully conducted, and the toxic time points of APAP, BB, CT, DMN, and TA were estimated as 12, 24, 6, 48, and 24 h, respectively. The maximal toxic times of BB (Chakrabarti and Brodeur, 1984), DMN (Asakura *et al.*, 1998), and TA (Wang *et al.*, 2000; Zaragoza *et al.*, 2000, respectively) in rats were the same as previously reported. In the CT-administered rats, AST and ALT elevated significantly at 6 and 48 h in the present study, but the CT toxicity assessed by serum AST and ALT increased at 6 to 24 h (AST) or 6 to 36 h (ALT) in a time-dependent manner, respectively (Zimmerman, 1999). In APAP-administered rats, AST and ALT elevated significantly at 6 and 12 h, but the serum AST and ALT were previously reported to be evaluated at 24 h by APAP administration (Hong *et al.*, 1992; Wang *et al.*, 1999). In the present study, the biochemical markers reflected the major gene expression profiles (Figs. 2, 3, 4, and 5).

We performed hierarchical clustering using gene groups whose expression levels were distinctively changed at the toxic time points (Fig. 1). At the maximal toxic time, CT and TA were sorted in a relatively close cluster. At the maximal toxic time, BB and DMN were sorted in a similar cluster. However, all APAP-administered groups were sorted in a different cluster. We performed many other types of hierarchical clustering by using other gene groups such as enzymes, signal transductions, and so on, and the results were almost the same as shown in Figure 1 (data not shown). Although studies concerning many hepatotoxicants including APAP, BB, CT, DMN, and TA administered to Sprague-Dawley rats have been reported (Kier *et al.*, 2004, McMillian *et al.*, 2004a,b), there has been no attempt of such a hierarchical clustering analysis using five chemicals. Thus, that the gene expression profiles of APAP administration were different from other those of the four chemicals constitutes new information.

In handling microarray data, it is necessary to consider what kinds of effects are relevant to the purpose of the experiments.

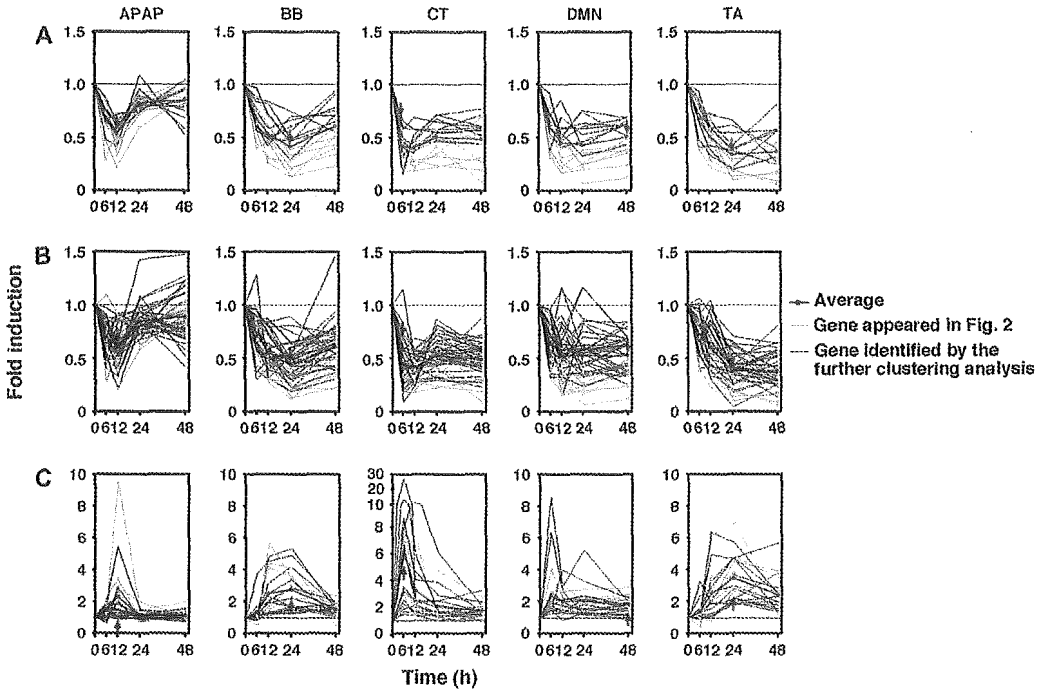

FIG. 5. Gene expression profiles of each group of chemical-administered rats identified by QT clustering analysis. The blue lines show the expression profiles of the genes that appeared in Figure 2. The red lines indicate the average of the expression. The red arrows indicate the maximal toxic time in each chemical-administered group estimated from the change of biochemical markers. (A) The expression profiles of genes down-regulated in the five chemical-administered groups. The expression profiles of genes that did not appear in Figure 2 are indicated by black lines. (B) The expression profiles of genes down-regulated in four of five chemical-administered groups. (C) The expression profiles of genes up-regulated in four of five chemical-administered groups. The expression profiles of the clustered genes that did not appear in Figure 2 are indicated by black lines. The analysis setting for the correlation coefficient was 0.65 and contained more than 10 genes.

We identified 20 representative genes whose up- or down-regulation peaks overlapped with the maximal toxic time (Fig. 2). In each of the chemical-administered rats, almost all genes identified in the present study showed similar expression profiles. The expression profile was confirmed in five representative genes, resulting in the overlapped profile with that of DNA microarray. Moreover, 17 of 20 genes were also identified by QT clustering analysis (Fig. 5). Data from QT clustering are independent of the hepatotoxicity estimated by serum biochemical markers. The present results showed the potential usefulness of 17 identified genes as toxicity markers. Most of the identified genes were not described previously as having a relationship with hepatotoxic chemicals. For example, TA administration up-regulated rat aldorase A mRNA (Bulera *et al.*, 2001). CtsL was up-regulated at the hepatic mRNA level after 24 h in BB- and TA-administered rats (Heijne *et al.*, 2003; Bulera *et al.*, 2001, respectively). Hmox1 was reported to be up-regulated by four chemicals, APAP (Chiu *et al.*, 2002), BB (Heijne *et al.*, 2003), CT (Montosi *et al.*, 1998), and TA (Bulera *et al.*, 2001; Matsuura *et al.*, 1988), in rats *in vivo*. In the present study, the expression of CYP2E1, which possibly catalyzes the induced toxicity of the five chemicals (Jeong, 1999; Lauriault *et al.*, 1992; Wang *et al.*, 2000; Zimmerman, 1999) was only slightly changed (data not shown), suggesting that the induction of CYP2E1 would not be involved.

QT clustering analysis is usually performed to determine the specific gene expression patterns. The resulting clusters gave us a good indication of the types of gene expression patterns that existed in the data (Heyer *et al.*, 1999). The gene expression patterns obtained from QT clustering analysis were major patterns expressed with each type of chemical administration (Fig. 4A). However, the extent of toxicity estimated by serum biochemical markers was different for each chemical. The average of each gene expression profile from QT clustering was overlapped with the changes of the serum biochemical markers. Furthermore, we performed QT clustering using Agilent Rat cDNA microarray kit G4105A in APAP-administered rat samples, the results of which showed almost the same expression profile (Fig. 4B). From this cDNA microarray, we confirmed the reproducibility of the new QT clustering data.

In conclusion, we identified 17 potential toxicity markers. It was not clarified whether all of the genes were related to the development of toxicity or whether these genes were related to each other. In the present study, we found that the expression profile analysis of the chemical administration could be used to estimate the maximal toxic time independently of the toxicity

grade. This expression profile analysis could also be a tool for identifying potential hepatotoxicants. This would be a new approach for determining hepatotoxicity by microarray analysis. We demonstrated that these two approaches, serum biochemical markers and two different QT clustering analyses, yielded the same results. For further studies, detailed time courses, multidose levels, and evaluation of other hepatotoxicants will be performed.

SUPPLEMENTARY DATA

Supplementary data are available online at www.toxsci.oxfordjournals.org.

ACKNOWLEDGMENTS

This work was supported in part by a grant from the Ministry of Education, Science, Sports, and Culture of Japan, and by Research on Advanced Medical Technology, Health and Labor Science Research Grants from the Ministry of Health, Labor and Welfare of Japan. We thank Mr. Brent Bell for reviewing the manuscript.

REFERENCES

Asakura, S., Daimon, H., Sawada, S., and Sagami, F. (1998). A short-term assessment of tumor-promotion activity in the livers of rats treated with two genotoxic methylating agents: Dimethylnitrosamine and methylnitrosourea. *Toxicol. Lett.* **98,** 155–167.

Bulera, S. J., Eddy, S. M., Ferguson, E., Jatkoe, T. A., Reindel, J. F., Bleavins, M. R., and De La Iglesia, F. A. (2001). RNA expression in the early characterization of hepatotoxicants in Wistar rats by high-density DNA microarrays. *Hepatology* **33,** 1239–1258.

Chakrabarti, S., and Brodeur, J. (1984). Dose-dependent metabolic excretion of bromobenzene and its possible relationship to hepatotoxicity in rats. *J. Toxicol. Environ. Health* **14,** 379–391.

Chiu, H., Brittingham, J. A., and Laskin, D. L. (2002). Differential induction of heme oxygenase-1 in macrophages and hepatocytes during acetaminophen-induced hepatotoxicity in the rat: Effects of hemin and biliverdin. *Toxicol. Appl. Pharmacol.* **181,** 106–115.

Dyroff, M. C., and Neal, R. A. (1981). Identification of the major protein adduct formed in rat liver after thioacetamide administration. *Cancer Res.* **41,** 3430–3435.

Heijne, W. H., Stierum, R. H., Slijper, M., van Bladeren, P. J., and van Ommen, B. (2003). Toxicogenomics of bromobenzene hepatotoxicity: A combined transcriptomics and proteomics approach. *Biochem. Pharmacol.* **65,** 857–875.

Heyer, L. J., Kruglyak, S., and Yooseph, S. (1999). Exploring expression data: Identification and analysis of coexpressed genes. *Genome Res.* **11,** 1106–1115.

Hong, R. W., Rounds, J. D., Helton, W. S., Robinson, M. K., and Wilmore, D. W. (1992). Glutamine preserves liver glutathione after lethal hepatic injury. *Ann. Surg.* **215,** 114–119.

Hughes, T. R., Mao, M., Jones, A. R., Burchard, J., Marton, M. J., Shannon, K. W., Lefkowitz, S. M., Ziman, M., Schelter, J. M., Meyer, M. R., *et al.* (2001). Expression profiling using microarrays fabricated by an ink-jet oligonucleotide synthesizer. *Nat. Biotech.* **19,** 342–347.

Hunter, A. L., Holscher, M. A., and Neal, R. A. (1977). Thioacetamide-induced hepatic necrosis. I. Involvement of the mixed-function oxidase enzyme system. *J. Pharmacol. Exp. Ther.* **200,** 439–448.

Jeong, H. G. (1999). Inhibition of cytochrome P450 2E1 expression by oleanolic acid: Hepatoprotective effects against carbon tetrachloride-induced hepatic injury. *Toxicol. Lett.* **105,** 215–222.

Kier, L. D., Neft, R., Tang, L., Suizu, R., Cook, T., Onsurez, K., Tiegler, K., Sakai, Y., Ortiz, M., Nolan, T., *et al.* (2004). Applications of microarrays with toxicologically relevant genes (tox genes) for the evaluation of chemical toxicants in Sprague Dawley rats *in vivo* and human hepatocytes *in vitro*. *Mutat. Res.* **549,** 101–113.

Lauriault, V. V., Khan, S., and O'Brien, P. J. (1992). Hepatocyte cytotoxicity induced by various hepatotoxins mediated by cytochrome P-450IIE1: Protection with diethyldithiocarbamate administration. *Chem. Biol. Interact.* **81,** 271–289.

Luo, L., Salunga, R. C., Guo, H., Bittner, A., Joy, K. C., Galindo, J. E., Xiao, H., Rogers, K. E., Wan, J. S., Jackson, M. R., *et al.* (1999). Gene expression profiles of laser-captured adjacent neuronal subtypes. *Nat. Med.* **5,** 117–122.

Matsuura, Y., Fukuda, T., Yoshida, T., and Kuroiwa, Y. (1988). Inhibitory effect of zinc-protoporphyrin on the induction of heme oxygenase and the associated decrease in cytochrome P-450 content in rats. *Toxicology* **50,** 169–180.

McMillian, M., Nie, A. Y., Parker, J. B., Leone, A., Bryant, S., Herlich, J., Yieh, L., Bittner, A., Liu, X., Wan, J., *et al.* (2004a). Inverse gene expression patterns for macrophage activating hepatotoxicants and peroxisome proliferators in rat liver. *Biochem. Pharmacol.* **67,** 2141–2165.

McMillian, M., Nie, A. Y., Parker, J. B., Leone, A., Bryant, S., Kemmerer, M., Herlich, J., Liu, Y., Yieh, L., Bittner, A., *et al.* (2004b). A gene expression signature for oxidant stress/reactive metabolites in rat liver. *Biochem Pharmacol.* **68,** 2249–2261.

Montosi, G., Garuti, C., Iannone, A., and Pietrangelo, A. (1998). Spatial and temporal dynamics of hepatic stellate cell activation during oxidant-stress-induced fibrogenesis. *Am. J. Pathol.* **152,** 1319–1326.

Price, V. F., and Jollow, D. J. (1982). Increased resistance of diabetic rats to acetaminophen-induced hepatotoxicity. *J. Pharmacol. Exp. Ther.* **220,** 504–513.

Sato, C., and Izumi, N. (1989). Mechanism of increased hepatotoxicity of acetaminophen by the simultaneous administration of caffeine in the rat. *J. Pharmacol. Exp. Ther.* **248,** 1243–1247.

Theocharis, S. E., Margeli, A. P., Skaltsas, S. D., Spiliopoulou, C. A., and Koutselinis, A. S. (2001). Induction of metallothionein in the liver of carbon tetrachloride intoxicated rats: An immunohistochemical study. *Toxicology* **161,** 129–138.

Wang, T., Shankar, K., Ronis, M. J., and Mehendale, H. M. (2000). Potentiation of thioacetamide liver injury in diabetic rats is due to induced CYP2E1. *J. Pharmacol. Exp. Ther.* **294,** 473–479.

Wang, P. Y., Kaneko, T., Wang, Y., and Sato, A. (1999). Acarbose alone or in combination with ethanol potentiates the hepatotoxicity of carbon tetrachloride and acetaminophen in rats. *Hepatology* **29,** 161–165.

Zaragoza, A., Andres, D., Sarrion, D., and Cascales, M. (2000). Potentiation of thioacetamide hepatotoxicity by phenobarbital pretreatment in rats. Inducibility of FAD monooxygenase system and age effect. *Chem. Biol. Interact.* **124,** 87–101.

Zimmerman, H. J. (1999). *Hepatotoxicity: The Adverse Effects of Drugs and Other Chemicals on the Liver*, 2nd ed., pp. 229–274. Lippncott Williams & Wilkins, Philadelphia.

Available online at www.sciencedirect.com
SCIENCE DIRECT®
ELSEVIER
Toxicology 216 (2005) 15–23
TOXICOLOGY
www.elsevier.com/locate/toxicol

Detection of autoantibody to aldolase B in sera from patients with troglitazone-induced liver dysfunction

Rawiwan Maniratanachote [a], Ayaka Shibata [a], Shuichi Kaneko [b], Ikuo Yamamori [c], Takanobu Wakasugi [d], Takeshi Sawazaki [e], Kanefusa Katoh [f], Shogo Tokudome [g], Miki Nakajima [a], Tsuyoshi Yokoi [a,*]

[a] *Division of Drug Metabolism, Faculty of Pharmaceutical Sciences, Kanazawa University, Kanazawa 920-1192, Japan*
[b] *Graduate School of Medicine, Kanazawa University, Kanazawa 920-0934, Japan*
[c] *Nagoya First Red-Cross Hospital, Nagoya 453-0046, Japan*
[d] *Fukui Prefectural Hospital, Fukui 910-8526, Japan*
[e] *Hitachi Chemical Co. Ltd., Hitachi 317-8555, Japan*
[f] *Institute for Developmental Research, Aichi Human Service Center, Kasugai, Aichi 480-0392, Japan*
[g] *Dokkyo University School of Medicine, Tochigi 321-0293, Japan*

Received 31 May 2005; received in revised form 13 July 2005; accepted 13 July 2005
Available online 22 August 2005

Abstract

Troglitazone is a thiazolidinedione antidiabetic agent with insulin-sensitizing activities that was withdrawn from the market in 2000 due to its association with idiosyncratic hepatotoxicity. To address the suspected autoantibody production associated with troglitazone, we investigated autoantibodies in sera from patients with type II diabetes mellitus with troglitazone-induced liver dysfunction. Two female patients (47- and 70-year-old) ceased taking troglitazone (400 mg/day) after 23.5 and 16 weeks, respectively, due to increased serum ALT. Using two-dimensional electrophoresis and amino acid sequence analyses, aldolase B was identified as an autoantigen that reacted with antibodies in sera from both patients. The titer of anti-aldolase B remained high for several weeks after stopping troglitazone administration. The mean reactivity of autoantibodies to aldolase B determined by ELISA with sera of patients with chronic hepatitis ($n=40$) and liver cirrhosis ($n=40$) was significantly higher ($p<0.05$ and $p<0.001$, respectively) than with sera of healthy subjects ($n=80$). These findings suggest that liver injury may cause the appearance of autoantibodies to aldolase B which may then aggravate the hepatitis. In addition, the anti-aldolase B titer might indicate the severity of liver dysfunction.

Keywords: Autoantibody; Aldolase B; Troglitazone; Thiazolidinediones; Liver dysfunction

1. Introduction

Adverse drug reactions can be classified into two basic types, reactions that occur directly and can be predicted from the pharmacology of the drug and, in contrast, idiosyncratic reactions which are induced dose-independently and are infrequent and unpredictable. Many idiosyncratic drug reactions have an immunological (hypersensitivity) basis, whereas some are due to a metabolic abnormality of the host (Ju and Uetrecht, 2002; Pirmohamed et al., 1998; Pohl et al., 1988). The liver is an important target for the toxic effects of drugs

* Corresponding author. Tel.: +81 76 234 4407; fax: +81 76 234 4407.
E-mail address: TYOKOI@kenroku.kanazawa-u.ac.jp (T. Yokoi).

0300-483X/$ – see front matter © 2005 Elsevier Ireland Ltd. All rights reserved.
doi:10.1016/j.tox.2005.07.012

because of its essential role in the metabolism of xenobiotic substances. Idiosyncratic drug-induced hepatitis has been assumed to be mediated by immunogens formed by covalent interaction of a reactive drug metabolite with cellular macromolecules (Ju and Uetrecht, 2002; Park et al., 1998). The bioactivated immunogens may not only lead to an immune response directed against the haptenic epitope and the neoantigen, but also against autoantigenic determinants, which is characterized by the formation of autoantibodies (Pohl et al., 1988). A number of hepatotoxic drugs have been reported to produce autoantibodies. For instance, anti-protein disulfide isomerase, anti-microsomal carboxyesterase, anti-calreticulin, anti-ERp72, anti-GRP78, anti-GRP94 and anti-CYP2E1 in halothane hepatitis (Bourdi et al., 1996; Gut et al., 1993; Kenna et al., 1993; Pumford et al., 1993), anti-CYP2C9 in tienilic acid-induced hepatitis (Homberg et al., 1984; Robin et al., 1996), anti-CYP1A2 in dihydralazine-induced hepatitis (Bourdi et al., 1990), and anti-CYPs in aromatic anticonvulsant-induced hypersensitivities (Leeder et al., 1992). However, it is not known whether the autoantibodies are the cause or consequence of the progression of hepatotoxicity. Studies to clarify the possible involvement of autoantibodies in drug-induced hepatitis have been limited, since the appearance of autoantibodies can be seen usually only in human (Descotes, 2000).

Troglitazone (Noscal®, Sankyo, Tokyo, Japan or Rezulin®, Parke-Davis, Morris Plains, NJ) was an early member of the thiazolidinedione chemicals developed for type II diabetes. It has a novel mechanism of action on lowering the blood glucose level by increasing glucose uptake by skeletal muscles, decreasing hepatic glucose production, and sensitizing target tissues to insulin (Fujiwara et al., 1995, 1988; Ciaraldi et al., 1990). However, a rare type of hepatic injury has been reported to be associated with troglitazone therapy. During clinical trials, 1.9% of patients experienced increases in ALT levels greater than three times the upper normal limit (Watkins and Whitcomb, 1998). Fulminant hepatic failure in some patients was reported to occur after long-term troglitazone treatment (more than 4 weeks) (Gitlin et al., 1998; Kuramoto et al., 1998; Neuschwander-Tetri et al., 1998; Shibuya et al., 1998). The hepatic toxicity of troglitazone was not observed in any experimental animals tested including monkey, which has a similar metabolic profile to human (Rothwell et al., 2002; Watanabe et al., 1999). Although the mechanism by which troglitazone causes liver dysfunction in certain individuals is not yet clear, it is thought to be idiosyncratic. There is no report so far of whether a metabolic idiosyncrasy or immunological idiosyncrasy causes this hepatotoxicity.

In the present study, we identified aldolase B as an autoimmune antigen which reacted against antibodies in sera of patients with troglitazone-induced liver dysfunction. The titer of the aldolase B autoantibody remained high for several weeks after stopping troglitazone administration. In addition, we also investigated the formation of the aldolase B autoantibodies in patients with chronic hepatitis and liver cirrhosis as compared with healthy subjects.

2. Materials and methods

2.1. Materials

Biotinylated anti-human IgG, biotinylated anti-rabbit IgG, and a VECTASTAIN ABC kit were purchased from Vector Labolatories Inc. (Burlingame, CA). Prestained SDS–polyacrylamide gel electrophoresis (PAGE) standard of low molecular weight range and prestained isoelectric point (p*I*) marker for two-dimensional PAGE were from Bio-Rad (Hercules, CA). 3,3′-Diaminobenzidine tetrahydrochloride (DAB) and 3,3′,5,5′-tretramethylbenzidine (TMB) liquid substrate system were from Sigma (St. Louis, MO). HRP conjugated anti-human IgA, IgG, IgM, kappa, lambda was from DakoCytomation (Glostrup, Denmark). Immobilon-P membrane was from Millipore (Bedford, UK). Ampholine was from Amersham Biosciences (Buckinghamshire, UK). Purified human aldolase B protein was previously prepared by Haimoto et al. (1989). Recombinant human aldolase B was a generous gift from Prof. Dean R. Tolan (Boston University, Boston, MA). Other chemicals were of the highest grade commercially available.

2.2. Patients

This study was approved by the Ethics Committee of Kanazawa University, Nagoya First Red-Cross Hospital, and Fukui Prefectural Hospital, Japan. The two patients (A and B) gave written informed consent. Serum ALT was periodically measured throughout the time of monitoring. Patient A was a 47-year-old Japanese female with diabetes mellitus. She had been prescribed insulin (36 U/day) for 3 years. Because of inadequate control of the blood sugar level, administration of insulin was stopped and troglitazone therapy (400 mg/day) was started in 1998. Sixteen weeks after the start of troglitazone therapy, the serum ALT level started to increase (32 IU/L). Since the serum ALT level had prominently increased to 229 IU/L at 23.5 weeks, troglitazone therapy was stopped (Fig. 1A). The serum ALT levels gradually decreased (183 IU/L, week 24; 113 IU/L, week 26; 24 IU/L, week 30; 12 IU/L, week 75). Patient B was a 70-year-old Japanese female with diabetes mellitus, hyperlipidemia, and essential hypertension. The patient had been prescribed glibenclamide (10 mg/day), pravastatin (10 mg/day), and celiprolol (100 mg/day). In 1998, because of inadequate control of the blood sugar level, troglitazone therapy was started at

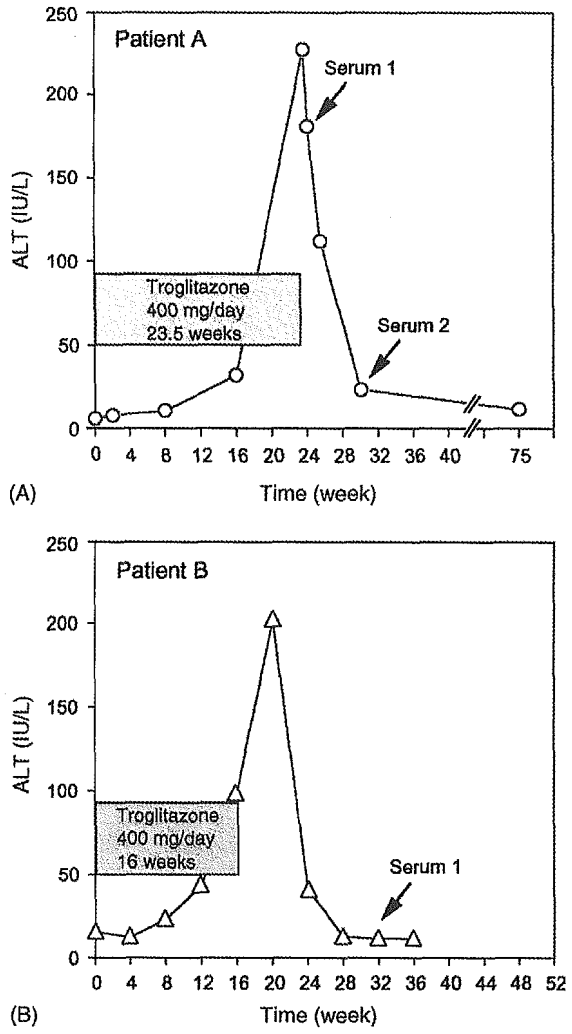

Fig. 1. Changes of serum ALT in patients with troglitazone-induced liver dysfunction. (A) Patient A (female, 47-year-old) and (B) patient B (female, 70-year-old) were administered troglitazone (400 mg/day) for 23.5 and 16 weeks, respectively. During the time of monitoring, the serum ALT of these patients was periodically measured at Fukui Prefectural Hospital and Nagoya First Red-Cross Hospital, Japan. Serum 1 and 2 of patient A and serum 1 of patient B were used in the further study.

400 mg/day. Eight weeks after the start of troglitazone therapy, the serum ALT level started to increase (24 IU/L). Since the serum ALT level continued to increase (44 IU/L, week 12; 99 IU/L, week 16), the troglitazone therapy was stopped (Fig. 1B). Although the serum ALT level had reached 205 IU/L at 20 weeks, the level subsequently decreased to normal (13 IU/L) at week 28.

Serum samples of 80 in-patients with liver dysfunction, 22 males and 18 females with chronic hepatitis, and 18 males and 22 females with liver cirrhosis, were obtained from Kanazawa University Hospital, Kanazawa, Japan. Serum samples of 80 healthy subjects, 45 males and 35 females, were obtained from the Red Cross Blood Supply Center, Kanazawa, Japan. The sera from healthy subjects were negative for serological tests of recent infection with hepatitis A and B viruses, cytomegalovirus and Epstein-Bar virus. All samples were stored at −20 °C until analysis.

2.3. Preparation of liver subcellular fractions

For immunoblot analysis, human liver samples were obtained from autopsy. The use of the human liver for the study was approved by the Ethics Committee of Dokkyo University School of Medicine (Tochigi, Japan). Liver tissues were rapidly frozen in liquid nitrogen immediately after excision and were stored at −80 °C. Human liver samples from two individuals (54-year-old male and 60-year-old female, ischemia cardionecrosis) were homogenized with 3 volumes of 0.1 M Tris–HCl (pH 7.4), 0.1 M KCl and 1 mM EDTA. Nuclei fractions were isolated by centrifugation at 600 × *g* for 10 min. The supernatant was centrifuged at 9000 × *g* for 20 min to isolate the mitochondria fraction. The supernatant was centrifuged at 105,000 × *g* for 60 min to prepare the microsome and cytosol fractions. The prepared fractions of nuclei, mitochondria, and microsomes were washed two times using the same experimental procedures. The protein concentration was measured according to the method of Lowry et al. (1951) with bovine serum albumin as a standard. The prepared subcellular fractions were stored at −80 °C until use.

2.4. Sodium dodecyl sulphate–polyacrylamide gel electrophoresis (SDS–PAGE) and immunoblot analysis

SDS–PAGE and immunoblot analysis were carried out. In brief, human liver homogenates (20 μg), nuclei (10 μg), mitochondria (10 μg), microsomes (10 μg), and cytosol (10 μg) were applied to 7.5% polyacrylamide gel. Proteins were transferred to an Immobilon-P membrane. The membrane was incubated with serum from healthy subjects, patient A or B (diluted 1:100) as the first antibody at 37 °C for 60 min. Subsequently, the membrane was incubated with biotinylated anti-human immunoglobulin (diluted 1:2000) at 37 °C for 30 min and incubated with avidin–biotin complex (VECTASTAIN ABC kits) at 37 °C for 30 min. Anti-sera to the human aldolase B raised in rabbit as described previously (Haimoto et al., 1989) was used (final concentration: 0.1 μg/ml) at 37 °C for 30 min. The membrane was incubated with biotinylated anti-rabbit IgG (diluted 1:2000) at 37 °C for 20 min and then with avidin–biotin complex (VECTASTAIN ABC kit) at 37 °C for 20 min. 3,3′-Diaminobenzidinetetrahydrochloride (DAB) was used as a substrate for peroxidase.

2.5. Two-dimensional electrophoresis

Two-dimensional electrophoresis was carried out according to the method described by O'Farrell (1975) with slight modifications. Isoelectric focusing (IEF) gel was prepared from a mixture containing 8 M urea, 2% Nonidet P-40, 2% Ampholines carrier ampholites (0.5% pH 6.0–8.0 range, 1.5% pH

7.0–9.0 range), and 4% acrylamide. Prefocusing was carried out at 200 V for 15 min, 300 V for 20 min, and then 400 V for 20 min. Samples up to 50 μl in volume were subjected to electrophoresis at 400 V for 12–16 h and at 800 V for 1 h using 0.02 M NaOH at the anode and 0.01 M H_3PO_4 at the cathode. The second dimensional separation was carried out using the 7.5% SDS–PAGE as described above.

2.6. Amino acid sequence analysis

After the two-dimensional electrophoresis, the separated proteins were visualized by staining with Coomassie Brilliant Blue G-250 (CBB). The corresponding spots of interest were compared with the profile from the immunoblotting with the patient A serum sample. The stained 40 kDa spots with p*I*s of 7.4 and 7.6 were excised and subjected to trypsin digestion. The analysis of peptides was carried out at APRO Science Inc. (Tokushima, Japan) by nanoflow ESI on a Q-TOF mass spectrometer.

2.7. Enzyme-linked immunosorbent assay (ELISA)

The sera of patient A (serum 2), the healthy subjects ($n = 80$), and those with chronic hepatitis ($n = 40$) and liver cirrhosis ($n = 40$) were subjected to ELISA. Recombinant human aldolase B purified from *E. coli* DH5α expressing cells was used as an antigen. To avoid non-specific reactions with the bacterial antigens, all human sera were pre-absorbed with *E. coli* DH5α lysate 1:2 (v/v) for 4 h at room temperature with agitation and were centrifuged at 10,000 rpm for 15 min at 4 °C.

Hundred microlitres of human recombinant aldolase B (10 μg/ml) in carbonate/bicarbonate buffer, pH 9.6 were coated onto each well of flat-bottomed microtiter plates (Corning, NY) and incubated overnight at 4 °C. The wells were washed three times with wash solution (50 mM Tris, 0.14 M NaCl, 0.05% Tween 20, pH 8.0) and blocked with 150 μl of solution containing 50 mM Tris–HCl, 0.14 M NaCl and 1% BSA, pH 8.0, at 37 °C for 2 h. After washing three times, 100 μl of sera (1:100) in the solution containing 50 mM Tris–HCl, 0.14 M NaCl, 0.1% BSA and 0.05% Tween 20, pH 8.0, were applied to each well and incubated at 37 °C for 1 h. Each plate included serum from patient A as a positive control. The wells were washed three times before adding HRP conjugated anti-human IgA, IgG, IgM, kappa, lambda (1:8000) in the same solution as for the serum dilution. The wells were incubated at 37 °C for 1 h, washed five times and 100 μl of tetramethyl benzidine (TMB) substrate solution were added to each well. After 30 min of incubation, the TMB reaction was stopped by adding 100 μl of 2 M H_2SO_4. The optical density was read at 450 nm by using a microtiter plate reader (Biotrak II, Amersham Biosciences). Controlled wells that were coated without aldolase B were also used for each serum sample. All assays were performed in triplicate and the specific binding of antibody to aldolase B in sera was calculated by subtracting the average absorbance of the control wells from the average absorbance of the aldolase B coated wells.

2.8. Statistical analysis

Data from ELISA were analyzed by Kruskal–Wallis nonparametric analysis of variance (ANOVA) followed by Dunn's multiple comparison test. $p < 0.05$ was considered significant.

3. Results

Immunoblot analyses were performed with human liver subcellular fractions using sera from healthy subjects and patients A and B. In order to investigate the existance of troglitazone-induced autoantibodies and to elucidate the subcellular localization of antigen proteins, human liver subcellular fractions from two different individuals were subjected to SDS–PAGE. Immunoblot analysis was performed using sera 1 of patients A and B (Fig. 1) as the first antibody. Immunostained bands of 55 kDa and 49 kDa molecular weight were observed in the serum of a healthy subject. The 55 kDa band was more intense than the 49 kDa band (Fig. 2). These bands could be detected in the sera of all healthy subjects examined ($n = 8$, data not shown). The serum of patient A recognized an intense band of 40 kDa and a faint band of 45 kDa in the cytosolic fraction, whereas a faint band of 40 kDa was detected with the serum of patient B (Fig. 2). The serum of a healthy control could not detect these 40 kDa and 45 kDa bands. Other minor bands in patients A and B sera showed low reproducibility. Thus,

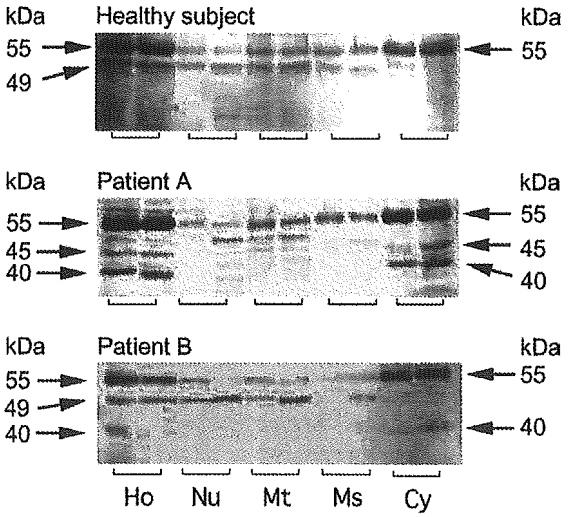

Fig. 2. Immunoblot analyses for human liver subcellular fractions using sera from healthy controls and patients A and B. Human liver homogenates (Ho), nuclei (Nu), mitochondria (Mt), microsomes (Ms), and cytosol (Cy) from two different individuals were subjected to SDS–PAGE. Immunoblot analyses were performed using sera from a healthy subject (1:100), patients A (serum 1, 1:100) and B (serum 1, 1:100) as the first antibody as described in Section 2.

we focused on the identification of the 40 kDa antigenic protein in further experiments.

In the serum of patient A, the immunoglobulin subtypes of antibody detecting the 55 kDa, 49 kDa, 45 kDa and 40 kDa proteins were IgG, IgM, IgG and IgG, respectively (data not shown). In the serum of patient B, the 55 kDa, 49 kDa and 40 kDa proteins were IgG, IgM and IgM, respectively (data not shown).

3.1. Two-dimensional electrophoresis of human liver cytosol and immunoblot analysis with the serum of patient A as the first antibody

To identify the 40 kDa antigenic protein, two-dimensional electrophoresis was carried out to analyze the liver cytosolic proteins. The separated proteins were stained with CBB (Fig. 3A). A relatively small number of protein spots were detectable due to the narrow pH range (pH 6–9) employed for the IEF. Immunoblot analysis using serum 1 of patient A as the first antibody indicated the presence of three 40 kDa antigenic proteins, whose estimated p*I*s were 7.6, 7.4 and 7.2 (Fig. 3B). The other immunostained spots seen on the membrane were assumed to be due to non-specific or non-immunological reactions with the serum. Spots of 55 kDa and 49 kDa were also observed on the immunostained membrane with the sera from the healthy subjects (data not shown).

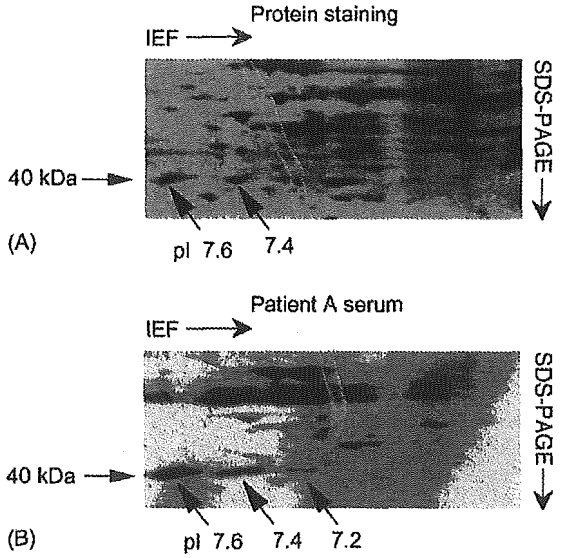

Fig. 3. Two-dimensional electrophoresis and immunoblot analyses using serum from patient A. Human liver cytosol (230 μg) was separated by two-dimensional electrophoresis. (A) The gel was stained with CBB. (B) Immunoblot analyses were performed using the serum 1 from patient A (1:100) as the first antibody as described in Section 2. The approximate p*I*s on the two-dimensional PAGE gel are indicated.

3.2. Identification of the 40 kDa antigenic protein

Two of the three immunoreactive spots with p*I*s of 7.6 and 7.4 in Fig. 3 were excised from the protein-stained two-dimensional PAGE gel and subjected to trypsin digestion. Amino acid sequencing was carried out with nanoflow ESI on a Q-TOF mass spectrometer. A 15-amino acid sequence (GGKAANKEATQEAFM) was identified from the trypsin-treated fragment of both spots. This sequence was perfectly matched with the amino acid sequence from 315 to 329 (GGKAANKEATQEAFM) of human aldolase B.

3.3. Confirmation of aldolase B by immunoblot analyses

To confirm that the 40 kDa protein was aldolase B, the following experiments were performed. To examine the possibility that the serum of patient A contained an antibody to aldolase B, purified human aldolase B protein (40 kDa) of 3 μg, 1 μg, and 0.25 μg were applied to SDS–PAGE and subsequently transferred to Immobilon-P membrane and immunostained with the serum of patient A as the first antibody. The serum 1 of patient A recognized the aldolase B in a concentration-dependent manner (Fig. 4A). The other serum of patient A (serum 2) and that of patient B (serum 1) showed the same immunological recognition of the purified aldolase B protein as that of serum 1 from patient A (data not shown).

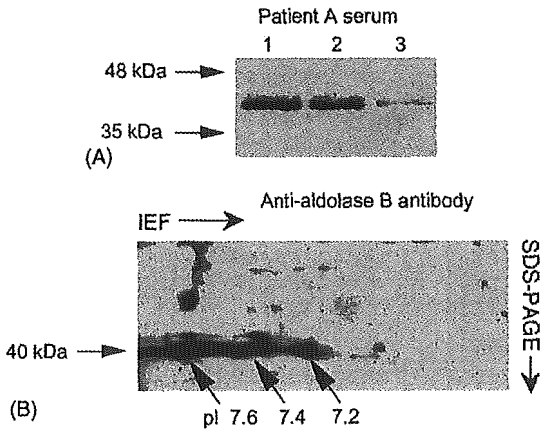

Fig. 4. Immunoblot analyses to confirm the occurrence of anti-aldolase B antibody. (A) Purified aldolase B protein at 3 μg (lane 1), 1 μg (lane 2), and 0.25 μg (lane 3) was subjected to SDS–PAGE. Immunoblot analysis was performed using serum 1 of patient A (1:100) as the first antibody. (B) Human liver cytosol (230 μg) was separated by two-dimensional electrophoresis. Immunoblot analysis was performed using anti-human aldolase B antibody as the first antibody as described in Section 2.

To examine the possibility that the spots recognized by immunostaining with the serum of patient A were derived from aldolase B, anti-human aldolase B antibody was applied instead of the serum of patient A to the liver cytosol prepared by two-dimensional PAGE. Three distinct spots with approximate p*I*s of 7.6 and 7.4, and 7.2, appeared (Fig. 4B). No other major spot was recognized by the anti-human aldolase B antibody. These spots showed the same p*I*s and molecular weights as the spots demonstrated by the serum of patient A.

To evaluate the titer of anti-aldolase B autoantibody in the sera of patients A and B the Immobilon-P membrane was employed to transfer the purified human aldolase B protein (1 μg). Immuoblot experiments were performed with the diluted sera from the patients. The sera 1 and 2 (23.5-week after stopping troglitazone therapy) of patient A showed titers of 1:3200 and 1:6400, respectively (data not shown). The titer of serum 1 (16-week after stopping troglitazone therapy) of patient B was 1:1600 (data not shown).

3.4. Determination of anti-aldolase B autoantibodies in sera of patients with liver diseases

The sera of the patients with liver diseases were examined by ELISA to determine whether the anti-aldolase B antibody appeared in association with the liver diseases. Fig. 5A shows the individual anti-aldolase B antibody in sera from the healthy subjects ($n=80$) and chronic hepatitis ($n=40$) and liver cirrhosis ($n=40$) patients. Anti-aldolase B autoantibodies in the chronic hepatitis and liver cirrhosis patients were significantly higher

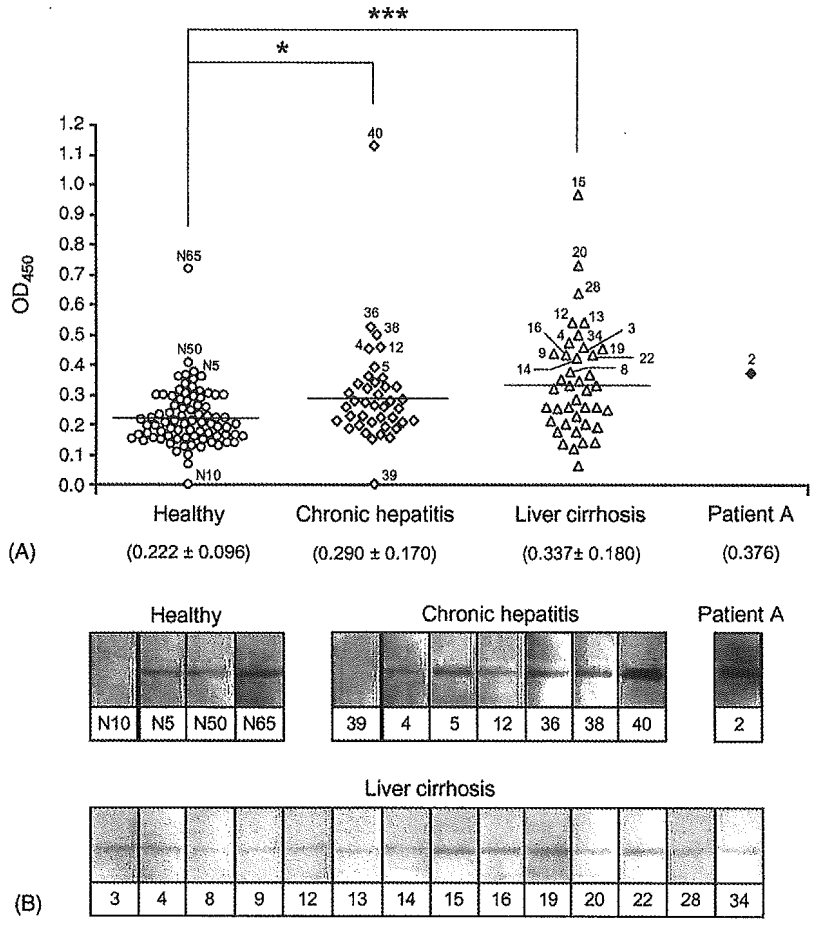

Fig. 5. Identification of autoantibodies reacting with aldolase B in sera from patients with liver diseases. (A) Sera of healthy subjects ($n=80$), chronic hepatitis ($n=40$) and liver cirrhosis ($n=40$) as well as patient A (positive control) were investigated for anti-aldolase B autoantibodies by ELISA as described in Section 2. The horizontal bar represents the average value of each group. The means ± S.D. are indicated in parentheses. $^{*}p<0.05$, $^{***}p<0.001$ compared with the control. (B) Immunoblot analyses of anti-aldolase B autoantibody positive sera. The sera which showed an OD_{450} higher than that of patient A, as well as negative sera from a healthy subject and chronic hepatitis, N10 and N39, respectively, were subjected to immunoblot analyses. The numbers correspond to the subjects indicated in (A).

than those in the healthy subjects ($p < 0.05$ and $p < 0.001$, respectively). Using serum 2 of patient A as a reference, all sera having an OD_{450} higher than that of patient A as well as negative sera from healthy subjects and those with chronic hepatitis, N10 and 39, respectively, were subjected to immunoblot analysis. Except the negative sera, all sera which showed positive reactivity by ELISA also showed a single positive band of aldolase B by immunoblotting (Fig. 5B).

4. Discussion

Idiosyncratic adverse reactions are difficult to study because of their rare occurrence, dose-independence and lack of reproducibility in animal models. There are two classes of reactions, metabolic and immunologic idiosyncrasy. The later class is thought to be responsible for most adverse drug reactions (Ju and Uetrecht, 2002; Pirmohamed et al., 1998; Pohl et al., 1988). In the present study, troglitazone-induced liver dysfunction was investigated in terms of the autoantibody formation. Two patients (A and B) who received troglitazone 400 mg/day showed increases of serum ALT (Fig. 1A and B), which indicated an abnormality of liver function. The sera of both patients reacted prominently against troglitazone-induced neoantigens in the cytosol subfraction (Fig. 2) which were identified as aldolase B (EC 4.1.2.13). Schapira et al. (1977) reported the microheterogeneity of human liver aldolase B, which shows 5 bands by IEF according to tetramers formed by two types of aldolase B chains, β and β′. The β′ chain is the result of a post-transcriptional modification by the deamidation of β chain. In our study, the spots of the two-dimensional PAGE at p*I* 7.6, 7.4, and 7.2 might be consistent with the β^4, $\beta^3\beta'$ and $\beta^2\beta'^2$ chains, respectively (Fig. 3). In mammal, three isoenzymes of aldolase (A–C) have been classified (Penhoet et al., 1966; Rutter, 1964). They are distinguished by their different activity towards the two substrates of fructose 1,6-diphospate and fructose 1-phosphate (Rutter et al., 1961). Aldolase B is predominantly localized in liver and kidney, while aldolase A and C are mainly localized in muscle and in brain, respectively (Penhoet et al., 1966; Rutter, 1964).

The mechanism by which autoantibodies are formed is still incompletely understood. Hepatic microsomal cytochrome P450 (CYP) isoforms such as CYP1A2, CYP2A6, CYP2B6, and CYP2E1 have been extensively studied as autoantigens in many liver diseases including viral, autoimmune and drug-induced hepatitis (Park et al., 1998; Manns and Obermayer-Straub, 1997). Although how these CYPs become autoimmune targets is still unknown, the findings of these studies reflected the major metabolic role of CYPs in the liver. However, in our findings no prominent band of CYPs could be detected in the microsomal subfraction of troglitazone-treated patient sera that was distinct from those in the sera of healthy subjects.

There is evidence that the metabolic activation of some drugs can result in the formation of chemically reactive metabolites that bind to macromolecules in the cell, unless adequately detoxified, leading to several pathological effects including hypersensitivities (Park et al., 1998). Thus, an imbalance between metabolic activation and detoxification in some individuals may lead to idiosyncratic adverse drug reactions. Troglitazone is metabolized by many enzymes in the liver including CYP3A4 and CYP2C8 which generated a quinone-type metabolite, troglitazone quinone (Tettey et al., 2001; Yamazaki et al., 1999). Based on the general involvement of quinones in cytotoxicity, troglitazone quinone has been proposed to have an association with troglitazone-induced hepatotoxicity (Neuschwander-Tetri et al., 1998). Aldolase B, which is an enzyme predominantly localized in the liver (Penhoet et al., 1966), may be one of the target proteins that interact with reactive species generated by troglitazone and trigger the immune response. Based on the detoxification enzyme in phase II, which is responsible for eliminating toxic metabolites before the generation of neoantigens, a recent report has shown that the double null genotype of *GSTM1* and *GSTT1* is associated with an abnormal elevation of liver enzymes caused by troglitazone treatment (Watanabe et al., 2003). This may suggest that idiosyncratic drug reactions might be the consequence of a complex genetic basis involving numerous processes.

In order to investigate whether the formation of anti-aldolase B was specific for troglitazone-induced hepatotoxicity, the sera of patients with liver diseases, chronic hepatitis and liver cirrhosis, were also examined. According to the etiology, chronic hepatitis results from several causes such as autoimmune reactions, viral hepatitis B–D, drugs, Wilson's disease, α-1-antitrypsin disease as well as unknown causes, whereas cirrhosis is considered to be the advanced stage of hepatitis (Batts and Ludwig, 1995; Jevon, 2001). As shown in Fig. 5, the mean reactivity of autoantibodies to aldolase B in the patient sera with liver diseases was also significantly higher than that in the healthy subjects. The average ALT level in chronic hepatitis and cirrhosis was 39.50 ± 15.7 IU/L ($n = 40$) and 52.35 ± 28.70 IU/L ($n = 40$), respectively (data not shown) which correlated with the titer of autoantibodies to aldolase B. Brown et al. (1987) reported that the presence of autoantibodies to aldolase in patients with hepatitis A, B, non-A/non-B,

and those who were hepatitis B surface antigen positive or had autoimmune hepatitis was higher than in healthy subjects. In that study, rabbit muscle aldolase, which is referred to as aldolase A (Penhoet et al., 1966), was used. According to the high homology between aldolase A and B, only the amino acid sequence 357–362 is recognized as a non-conserved residue that enables the classification of the mammalian aldolase (Rutter, 1964). The amino acid sequence 315–329 of aldolase B was identified in our study. Therefore, our findings were remarkably consistent with those of a previous report (Brown et al., 1987). In addition, we included the data of autoantibodies to aldolase B detected in troglitazone-induced hepatitis as well as those in liver cirrhosis.

At present, the exact mechanism involved in the formation of autoantibodies is unknown. There is a possibility that, after cellular injury, intracellular antigens might be seen as non-self by the immune system and result in the stimulation of an immune response toward cryptic epitopes on the antigens (Lanzavecchia, 1995). Accumulating evidence suggests that liver damage may cause the production of autoantibodies to aldolase B and that the severity of hepatitis may be estimated by the antibody titer.

In conclusion, aldolase B was identified as an autoimmune antigen in patients with troglitazone-induced liver dysfunction. This finding is the first evidence that troglitazone-induced hepatitis may have an immunological basis. In addition, the elevation of anti-aldolase B autoantibody in sera is likely a common phenomenon associated with hepatitis. This autoantibody may play an essential role in aggravating the liver dysfunction. Further studies will be needed to clarify the mechanisms of idiosyncratic adverse drug reactions.

Acknowledgements

We thank Prof. Dean R. Tolan, Boston University, Boston, MA, for providing recombinant human aldolase B. We also thank Mr. Brent Bell for reviewing the manuscript. This work was supported in part by a grant from the Ministry of Education, Science, Sports and Culture of Japan, and by Research on Advanced Medical Technology, Health and Labor Science Research Grants from the Ministry of Health, Labor and Welfare of Japan.

References

Batts, K.P., Ludwig, J., 1995. Chronic hepatitis. An update on terminology and reporting. Am. J. Surg. Pathol. 19, 1409–1417.

Bourdi, M., Chen, W., Peter, R.M., Martin, J.L., Buters, J.T., Nelson, S.D., Pohl, L.R., 1996. Human cytochrome P450 2E1 is a major autoantigen associated with halothane hepatitis. Chem. Res. Toxicol. 9, 1159–1166.

Bourdi, M., Larrey, D., Nataf, J., Bernuau, J., Pessayre, D., Iwasaki, M., Guengerich, F.P., Beaune, P.H., 1990. Anti-liver endoplasmic reticulum autoantibodies are directed against human cytochrome P-450IA2. A specific marker of dihydralazine-induced hepatitis. J. Clin. Invest. 85, 1967–1973.

Brown, C., Toh, B.H., Pedersen, J.S., Clarke, F.M., Mackay, I.R., Gust, I., 1987. Autoantibody to aldolase in acute and chronic hepatitis. Pathology 19, 347–350.

Ciaraldi, T.P., Gilmore, A., Olefsky, J.M., Goldberg, M., Heidenreich, K.A., 1990. In vitro studies on the action of CS-045, a new antidiabetic agent. Metabolism 39, 1056–1062.

Descotes, J., 2000. Autoimmunity and toxicity testing. Toxicol. Lett. 112–113, 461–465.

Fujiwara, T., Okuno, A., Yoshioka, T., Horikoshi, H., 1995. Suppression of hepatic gluconeogenesis in long-term troglitazone treated diabetic KK and C57BL/KsJ-db/db mice. Metabolism 44, 486–490.

Fujiwara, T., Yoshioka, S., Yoshioka, T., Ushiyama, I., Horikoshi, H., 1988. Characterization of new oral antidiabetic agent CS-045: Studies in KK and ob/ob mice and Zucker fatty rats. Diabetes 37, 1549–1558.

Gitlin, N., Julie, N.L., Spurr, C.L., Lim, K.N., Juarbe, H.M., 1998. Two cases of severe clinical and histologic hepatotoxicity associated with troglitazone. Ann. Intern. Med. 129, 36–38.

Gut, J., Christen, U., Huwyler, J., 1993. Mechanisms of halothane toxicity: novel insights. Pharmacol. Ther. 58, 133–155.

Haimoto, H., Kurobe, N., Hosoda, S., Kato, K., 1989. Sensitive enzyme immunoassay for human aldolase B. Clin. Chim. Acta 181, 27–36.

Homberg, J.C., Andre, C., Abuaf, N., 1984. A new anti-liver-kidney microsome antibody (andi-LKM2) in tienilic acid-induced hepatitis. Clin. Exp. Immunol. 55, 561–570.

Jevon, G.P., 2001. Grade and stage in chronic hepatitis. Pediatr. Dev. Pathol. 4, 372–380.

Ju, C., Uetrecht, J.P., 2002. Mechanism of idiosyncratic drug reaction: relative metabolites formation, protein binding and the regulation of the immune system. Curr. Drug Metab. 3, 367–377.

Kenna, J.G., Knight, T.L., van Pelt, F.N.A.M., 1993. Immunity to halothane metabolite-modified proteins in halothane hepatitis. Ann. N. Y. Acad. Sci. 685, 646–661.

Kuramoto, K., Shimizu, N., Toda, G., 1998. Liver dysfunction associated with troglitazone (Noscal®). Rinsho-Iyaku 14, 461–466.

Lanzavecchia, A., 1995. How can cryptic epitopes trigger autoimmunity? J. Exp. Med. 181, 1945–1948.

Leeder, J.S., Riley, R.J., Cook, V.A., Spielberg, S.P., 1992. Human anti-cytochrome P450 antibodies in aromatic anticonvulsant-induced hypersensitivity reactions. J. Pharmacol. Exp. Ther. 263, 360–367.

Lowry, O.H., Rosebrough, N.J., Farr, A.L., Randall, R.J., 1951. Protein measurement with the Folin phenol reagent. J. Biol. Chem. 193, 265–275.

Manns, M.P., Obermayer-Straub, P., 1997. Cytochromes P450 and uridinetriphosphate-glucuronosyltransferases: model autoantigens to study drug-induced, virus-induced and autoimmune liver disease. Hepatology 26, 1054–1066.

Neuschwander-Tetri, B.A., Isley, W.L., Oki, J.C., Ramrakhiani, S., Quiason, S.G., Phillips, N.J., Brunt, E.M., 1998. Troglitazone-induced hepatic failure leading to liver transplantation. Ann. Intern. Med. 129, 38–41.

O'Farrell, P.H., 1975. High resolution two-dimensional electrophoresis. J. Biol. Chem. 250, 4007–4021.

Park, B.K., Pirmohamed, M., Kitteringham, N.R., 1998. Role of drug disposition in drug hypersensitivity: a chemical, molecular and clinical perspective. Chem. Res. Toxicol. 11, 969–988.

Penhoet, E., Rajkumar, T., Rutter, W.J., 1966. Multiple forms of fructose diphosphate aldolase in mammalian tissues. Proc. Natl. Acad. Sci. U.S.A. 56, 1275–1282.

Pirmohamed, M., Breckenridge, A.M., Kitteringham, N.R., Park, B.K., 1998. Adverse drug reactions. Br. Med. J. 316, 1295–1298.

Pohl, L.R., Satoh, H., Christ, D.D., Kenna, J.G., 1988. The immunologic and metabolic basis of drug hypersensitivities. Ann. Rev. Pharmacol. 28, 367–387.

Pumford, N.R., Martin, B.M., Thomassen, D., Burris, J.A., Kenna, J.G., Martin, J.L., Pohl, L.R., 1993. Serum antibodies from halothane hepatitis patients react with the rat endoplasmic reticulum protein Erp72. Chem. Res. Toxicol. 6, 609–615.

Robin, M.A., Maratrat, M., Le Roy, M., Le Breton, F.P., Bonierbale, E., Dansette, P., Ballet, F., Mansuy, D., Pessayre, D., 1996. Antigenic targets in tienilic acid hepatitis: Both cytochrome P450 2C11 and 2C11-tienilic acid adducts are transported to the plasma membrane of rat hepatocytes and recognized by human sera. J. Clin. Invest. 98, 1471–1480.

Rothwell, C., McGuire, E.J., Altrogge, D.M., Masuda, H., de la Iglesia, F.A., 2002. Chronic toxicity in monkeys with the thiazolidinedione antidiabetic agent troglitazone. J. Toxicol. Sci. 27, 35–47.

Rutter, W.J., 1964. Evolution of aldolase. Fed. Proc. 23, 1248–1257.

Rutter, W.J., Richards, O.C., Woodfin, B.M., 1961. Comparative studies of liver and muscle aldolase. I. Effect of carboxypeptidase on catalytic activity. J. Biol. Chem. 236, 3193–3197.

Schapira, F., Gregori, C., Hatzfeld, A., 1977. Isoelectrofocusing of aldolase B from normal human livers and from livers with hereditary fructose intolerance. Clin. Chim. Acta 78, 1–8.

Shibuya, A., Watanabe, M., Fujita, Y., Saigenji, K., Kuwao, S., Takahashi, H., Takeuchi, H., 1998. An autopsy case of troglitazone-induced fulminant hepatitis. Diabetes Care 21, 2140–2143.

Tettey, J.N., Maggs, J.L., Rapeport, W.G., Pirmohamed, M., Park, B.K., 2001. Enzyme induction dependent bioactivation of troglitazone and troglitazone quinone in vivo. Chem. Res. Toxicol. 14, 965–974.

Watanabe, I., Tomita, A., Shimizu, M., Sugawara, M., Yasumo, H., Koishi, R., Takahashi, T., Miyoshi, K., Nakamura, K., Izumi, T., Matsushita, Y., Furukawa, H., Haruyama, H., Koga, T., 2003. A study to survey susceptible genetic factors responsible for troglitazone-associated hepatotoxicity in Japanese patients with type 2 diabetes mellitus. Clin. Pharmacol. Ther. 73, 435–455.

Watanabe, T., Ohashi, Y., Yasuda, M., Takaoka, M., Furukawa, T., Yamoto, T., Sanbuissho, A., Manabe, S., 1999. Was it possible to predict liver dysfunction caused by troglitazone during the nonclinical safety studies? Iyakuhin Kenkyu 30, 537–546.

Watkins, P.B., Whitcomb, R.W., 1998. Hepatic dysfunction associated with troglitazone. N. Engl. J. Med. 338, 916–917.

Yamazaki, H., Shibata, A., Suzuki, M., Nakajima, M., Shimada, N., Guengerich, F.P., Yokoi, T., 1999. Oxidation of troglitazone to a quinone-type metabolite catalyzed by cytochrome P-450 2C8 and P-450 3A4 in human liver microsomes. Drug Metab. Dispos. 27, 1260–1266.

Available online at www.sciencedirect.com
SCIENCE DIRECT®
ELSEVIER
Mutation Research 603 (2006) 64–73
Genetic Toxicology and Environmental Mutagenesis
www.elsevier.com/locate/gentox
Community address: www.elsevier.com/locate/mutres

Simultaneous measurement of gene expression for hepatotoxicity in thioacetamide-administered rats by DNA microarrays

Keiichi Minami, Rawiwan Maniratanachote, Miki Katoh, Miki Nakajima, Tsuyoshi Yokoi*

Drug Metabolism and Toxicology, Division of Pharmaceutical Sciences, Graduate School of Medical Science, Kanazawa University, Kanazawa 920-1192, Japan

Received 26 August 2005; received in revised form 26 September 2005; accepted 28 October 2005
Available online 5 December 2005

Abstract

DNA microarray technology was developed as a tool for simultaneously measuring a number of gene expression changes, and has been applied for investigations of toxicity assessments of chemicals. In this study, we used a typical hepatotoxicant, thioacetamide (TA), to find correlations between the extent of hepatotoxicity and certain gene expression patterns or specific gene expression profiles. TA was intraperitonealy administered at high (400 mg/kg), medium (150 mg/kg) or low (50 mg/kg) dose (four rats per group) and then the serum and liver were collected at the indicated time (6, 12, 24, 36 and 48 h). Serum biochemical markers were measured and hepatic mRNA expression profiles were analyzed by a DNA microarray. Serum aspartate aminotransferase (AST) and alanine aminotransferase (ALT) were increased by TA-administration in a dose-dependent manner and reached the maximum at 24 h. Hierarchical clustering analysis of all dosage groups revealed in 2 major clusters, distinguished by an early (6 and 12 h) and a late (24, 36 and 48 h) phase. The early and late phase clusters were sorted in time- and dose-dependent manners. The major gene expression profile obtained by quality-threshold (QT) clustering analysis showed the same maximal toxic time as that estimated by the serum biochemical markers. The individual expression profiles of the candidate genes selected in our previous studies and the simultaneous gene expression patterns measured by five typical hepatotoxicants including TA also reflected the hepatotoxicity of TA. These findings suggest that the potential toxic effects appearing as gene expression changes are independent of the dosage of TA. This study suggested that the major gene expression profile estimated by QT clustering would be a sensitive marker of hepatotoxicity.

Keywords: Gene expression profiles; Hepatotoxicity; DNA microarray

1. Introduction

The prediction of chemical-induced adverse effects on an organism is one of the aims of toxicology. In the past several years, a microarray technology has rapidly developed. Microarrays are available to assess both known and unknown genes in the experimental materials. Microarrays are also available to assess simultaneously the effects of various factors on the gene expression of all known sequences including expression sequence tags (ESTs) at the RNA level.

For microarray data assessment, several clustering methods are often used. Clustering places the data of interest into a small number of relatively homo-

* Corresponding author. Tel.: +81 76 234 4407; fax: +81 76 234 4407.
E-mail address: TYOKOI@kenroku.kanazawa-u.ac.jp (T. Yokoi).

1383-5718/$ – see front matter © 2005 Elsevier B.V. All rights reserved.
doi:10.1016/j.mrgentox.2005.10.008

geneous groups or clusters [1]. For example, there is hierarchical clustering expressed by a dendrogram, *K*-means clustering [2], and quality-threshold (QT) clustering [3]. These clustering methods are useful ways to extract and visualize one-to-one correlations. Microarray technology can be used as a tool for clarifying the mechanisms of chemical-induced toxicity, forecasting the adverse effects of drug candidates and improving the process of risk assessment and safety evaluation.

The liver is one of the first organs to be exposed when chemicals are administered perorally or via the portal vein. Chemical concentrations in the liver are often much higher than the peak plasma concentration. The liver is also the major site for metabolizing xenobiotics and these chemicals can lead to the formation of active metabolites. Thus, the liver is one of the primary targets for various types of chemical-induced toxicity. Therefore, investigating the gene expression changes and comparing the gene expression profiles to the extent of liver toxicity are useful for the assessment of liver toxicity.

To construct an animal model of liver toxicity, we chose thioacetamide (TA) as a potent hepatotoxicant that requires metabolic activation by mixed-function oxidases. TA is metabolized by cytochrome P450 (CYP) 2B, CYP2E1 and flavin-containing monooxygenase (FMOs) to its toxic metabolites [4,5] and these intermediate metabolites might bind to cellular proteins by the formation of acetylimidolysine derivatives [6]. The reactive metabolites responsible for TA hepatotoxicity are the radicals derived from thioacetamide-*S*-oxide and the reactive oxygen species derived as subproducts in the process of microsomal TA oxidation, both of which deplete reduced glutathione leading to oxidative stress [7–11].

The purpose of the present study is to determine the correlations between biochemical markers for hepatotoxicity and hepatic gene expression profiles at various doses of TA-administration in rats, and then to extrapolate the DNA microarray data for predicting hepatotoxic chemicals.

2. Materials and methods

2.1. Animals and chemicals

Male Sprague–Dawley rats (5-week old, 130–150 g) were obtained from SLC Japan (Hamamatsu, Japan). Animals were housed in the institutional animal facility in a controlled environment (temperature 25 ± 1 °C, humidity 50 ± 10% and 12 h light/12 h dark cycle) with access to food and water ad libitum. Animals were acclimatized for a week before use. Animal maintenance and treatment were conducted in accordance with the National Institutes of Health Guide for Animal Welfare of Japan, as approved by the Institutional Animal Care and Use Committee of Kanazawa University. TA (CAS No. 62-55-5) was obtained from Wako Pure Chemical Industries (Osaka, Japan). ISOGEN, RNA extraction reagent, was purchased from Nippon Gene (Tokyo, Japan). CodeLink™ Expression Assay Reagent kit, Manual Prep and streptavidin-Cy5 were from GE Healthcare Amersham Biosciences (Buckinghamshire, UK). The QIAquick PCR purification kit and a RNeasy mini kit were from Qiagen (Hilden, Germany). NEN Blocking Reagent and Biotin 11-UTP were from Perkin-Elmer Life Sciences (Boston, MA). ReverTra Ace (Moloney Murine Leukemia Virus Reverse Transcriptase RnaseH Minus) was from Toyobo (Tokyo, Japan). Random hexamer and SYBR® Premix Ex Taq™ (perfect real time) were from Takara (Osaka, Japan). All primers were commercially synthesized at Hokkaido System Sciences (Sapporo, Japan). Other chemicals were of the highest grade commercially available.

2.2. TA-administration and assessment of liver injury

Sixty-four rats were assigned to 16 groups (four rats/group). Rats received a single dose of TA dissolved in saline by intraperitoneal injection. The dosing solutions were prepared to deliver a volume of 2 ml/kg as follows; 400 mg/kg high dose, 150 mg/kg medium dose, 50 mg/kg low dose. At the indicated time (6, 12, 24, 36, and 48 h after the administration), blood samples were collected from the atrium, and then the rats were sacrificed and the liverscollected. Four typical biochemical markers for hepatotoxicity (aspartate aminotransferase, AST; alanine aminotransferase, ALT; lactate dehydrogenase, LDH; bilirubin) were measured by SRL (Tokyo, Japan).

2.3. RNA isolation

Total hepatic RNA was isolated using ISOGEN. Approximately 100 mg of whole liver were lysed with 1.0 ml of the reagent. Chloroform (200 μl) was added and vortexed vigorously for 15 s. The mixture was centrifuged at 15,000 × *g* for 15 min at 4 °C. The aqueous phase was transferred carefully to a new tube, and the RNA was precipitated with 0.5 ml of isopropyl alcohol for 10 min at room temperature. The mixture was centrifuged at 15,000 × *g* for 10 min. After washing with 75% ethanol, the pellet was dissolved in diethylpyrocarbonate-treated water. Equal amounts of total mRNA from samples of each administration were pooled and used for the microarray analysis and real-time reverse transcriptase (RT)-PCR.

2.4. Microarray analysis

Microarray experiments were performed using a CodeLink™ Bioarray Perfect System according to the manufacturer's protocol (GE Healthcare Amersham Biosciences). In this experiment, we used Codelink™ Uniset Rat

I Bioarray (GE Healthcare Amersham Biosciences) consisting of 9936 genes including ESTs. Processed slides were scanned with an Agilent G2565BA Microarray Scanner using Agilent Scan Control Software (Agilent Technologies, Palo Alto, CA) with the laser set to red (633 nm) and the photomultiplier tube (PMT) value to 70%. The scanned images for each slide were analyzed using the CodeLink™ Expression Analysis Software (GE Healthcare Amersham Biosciences). The microarray data quality control was as follows: present, no flags (neither marginal nor absent); marginal, low quality spots judged by analysis software; absent, low signal density spots.

2.5. Real-time RT-PCR

Rat V1a arginine vasopressin receptor (Avpr1a), cyclin G1 (Ccng1), growth arrest and DNA-damage-inducible 45alpha (Gadd45a), heme oxygenase 1 (Hmox1), L-3-hydroxyacyl-Coenzyme A dehydrogenase (Hadhsc), lysozyme (Lyz), sulfotransferase 1a2 (Sult1a2), T-cell death associated gene (Tdag) and GAPDH were quantified by real-time RT-PCR. Primer sequences used in this study were as follows: Avpr1a: 5′-TAC GTG ACC TGG ATG ACC AG-3′ and 5′-AGC AAC GCC GTG ATT GTG AT-3′ [12], Ccng1: 5′-CCT TCC AAT TTC TGC AGC TC-3′ and 5′-CTT GGA AAC AAG CTC TTG CC-3′ [13], Gadd45a: 5′-AAG ATC GAA AGG ATG GAC ACG-3′ and 5′-GTA GCA ACA GCT CTG CCA GC-3′ [14], Hmox1: 5′-ATA GAG CGA AAC AAG CAG A-3′ and 5′-TAG AGC TGT TTG AAC TTG G-3′, Hadhsc: 5′-TGC AGA TCA CAA ACA TAG CC-3′ and 5′-TCC AGT CCA ACA TAG TCA AG-3′, Lyz: 5′-CTC AAA CCA ACA GGG CTT TC-3′ and 5′-CCC AAG ATC AAC TCG TCT CC-3′ [15], Sult1a2: 5′-TCA TTG AGT GGA CTT TGC CTT-3′ and 5′-CAC TTT TCC AGC TTT GAA CTG-3′, Tdag: 5′-CCA AGC AGG TAC AAC ATC AG -3′ and 5′-TTC TGC CTC GTA GAC TTG AC-3′, GAPDH: 5′-GTT ACC AGG GCT GCC TTC TC-3′ and 5′-GGG TTT CCC GTT GAT GAC C-3′. For RT process, total RNA (4 μg) and 150 ng random hexamer were mixed and incubated at 70 °C for 10 min. The RNA solution was added to a reaction mixture containing 100 units of ReverTra Ace, reaction buffer and 0.5 mM dNTPs in a final volume of 40 μl. The reaction mixture was incubated at 30 °C for 10 min, 42 °C for 1 h and heated at 98 °C for 10 min to inactivate the enzyme. Real-time PCR was performed using the Smart Cycler® (Cepheid, Sunnyvale, CA) with Smart Cycler® software (Ver. 1.2b). The PCR mixture contained 1 μl of template cDNA, SYBR® Premix Ex Taq™ solution and 10 pmol of sense and antisense primers. The PCR condition for Ccng1, Sult1a2 and GAPDH was as follows: after an initial denaturation at 95 °C for 30 s, the amplification was performed by denaturation at 94 °C for 4 s, annealing and extension at 64 °C for 20 s for 45 cycles. The PCR condition for other six genes was as follows: after an initial denaturation at 95 °C for 20 s, the amplification was performed by denaturation at 95 °C for 5 s, annealing at 55 °C for 10 s and extension at 72 °C for 15 s for 45 cycles. The amplified products were monitored directly by measuring the increase of the dye intensity of the SYBR® Green I.

2.6. Data management

Microarray data management was performed with GeneSpring software (Agilent Technologies). Comparison of present genes, fold change determinations, experiment normalization and various clustering analyses were performed. The gene expression values for each array were normalized to their respective median value. All clustering analyses were performed using standard correlations. Fold change filters included the requirement that the genes be present in at least 200% of controls for up-regulated genes and lower than 50% of controls for down-regulated genes.

3. Results

3.1. Assessment of liver toxicity

The serum biochemical markers in the TA-administered groups were measured at 6, 12, 24, 36 and 48 h after administration (Fig. 1). The AST activities of all dosage groups were significantly high at 24 h. The changes of ALT activities were similar to those of the AST activities. The LDH activity increased significantly in the medium dose- and the high dose-administered groups at 24 h, but not in the low dose-administrated groups. No significant change of the unconjugated bilirubin was observed in any of the groups (data not shown), whereas conjugated bilirubin increased only in the 24 h high-dose group (0 h: 0 mg/dl, 24 h: 0.3 mg/dl). Taking these results into consideration, the maximal toxic times of each TA dosage were estimated as 24 h.

3.2. Two-way hierarchical clustering of gene expression profiles in TA-induced hepatotoxicity in rats

The mRNA expression profiles in the three dosage and five time points were determined using the data from the DNA microarray. Two-way hierarchical clustering was performed based on the expression profiles of the genes with a significant variation in the expression level across all the experiments. After cutting off the absent and marginal flags, 7978 out of 9936 genes were present in this experiment. The results are shown in a color-coded matrix (Fig. 2) where samples are ordered on the horizontal axis and genes on the vertical axis on the basis of the similarity of their expression profiles.

The administered groups were sorted into two large clusters that extensively differed with respect to an early phase (6 and 12 h; left cluster) or a late phase (24, 36 and 48 h; right cluster) (Fig. 2A). In the early phase cluster,

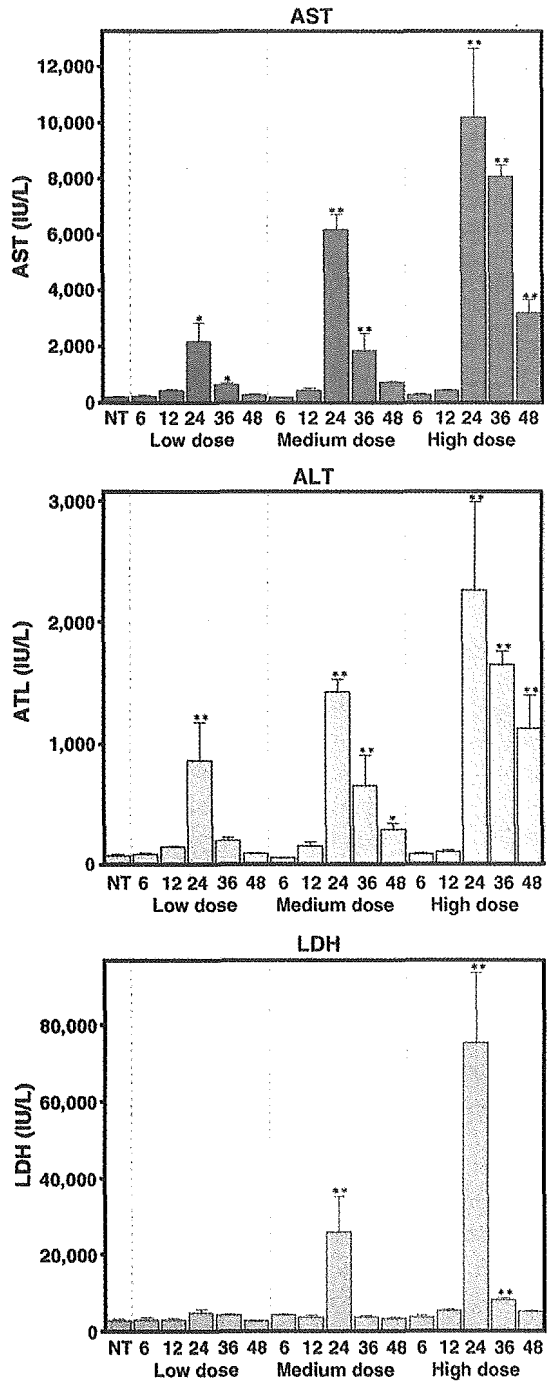

Fig. 1. Changes of AST, ALT and LDH in serum of TA-administered rats. TA was administered at high dose (400 mg/kg weight), medium dose (150 mg/kg weight) and low dose (50 mg/kg weight). Blood samples were collected at 6, 12, 24, 36, 48 h after administration. Data are expressed as mean ± S.E. from four rats. Significantly different from NT group ($^{*}p<0.05$, $^{**}p<0.01$). NT; non-treated.

Table 1
Classification of genes those expression were significantly changed in all TA-administered groups

Category	Total[a]	Present[b]	Up (%)	Down (%)
Apoptosis regulator	33	25	4 (16.0)	0 (0)
Cancer	51	28	3 (10.7)	0 (0)
Cell cycle regulator	25	19	2 (10.5)	1 (5.3)
Chaperone	33	19	1 (5.3)	2 (10.5)
Enzyme	852	657	24 (3.7)	100 (15.2)
Immunity protein	42	31	0 (0)	2 (6.5)
Microtublar protein	16	8	0 (0)	1 (12.5)
Nucleic acid binding	175	126	12 (9.5)	6 (4.8)
Other groups	102	71	2 (2.8)	1 (1.4)
RNA	2	1	0 (0)	0 (0)
Signal transducer	201	124	7 (5.6)	9 (7.3)
Storage	3	2	0 (0)	0 (0)
Structural protein	181	116	7 (6.0)	12 (10.3)
Transport	313	208	10 (4.8)	26 (12.5)
Total	2029	1435	72 (5.0)	160 (11.1)

Up-regulated gene showed more than 200% expression of control. Down-regulated gene showed less than 50% expression of control.
[a] Gene number those category were defined.
[b] Gene number showing enough spot density.

the 12 h-groups were sorted into small hierarchies. On the other hand, the late phase cluster groups were sorted in a dose-dependent manner except for the 24 h-group. Especially, all dosages in the 24 h-groups were categorized at the same level.

We also performed hierarchical clustering based on each dosage (Fig. 2B). The clusters were sorted in a similar pattern as shown in Fig. 2A. The distance between the early (6 and 12 h) and the late (24, 36 and 48 h) phase was increased in a time-dependent manner as shown in the dendrogram of each group (above the matrix, Fig. 2B).

3.3. Category classification of genes in TA-induced hepatotoxic Rats

To evaluate the gene expression pattern on the basis of gene function, we classified the genes whose expressions were significantly changed at all dosages in the 24 h groups (Table 1). Based on each gene annotation, 13 categories were classified. Based on the percentage and the gene numbers categorized by gene annotation, the genes in the apoptosis regulator and the nucleic acid binding category were typically up-regulated and the genes in the enzyme, structural protein and transport category were down-regulated (Table 1).